Starch from *Colocasia esculenta* (L.) Schott of purple and white esculenta varieties: Thermal, technological properties, and morphological study

Almidón de *Colocasia esculenta* (L.) Schott de variedades esculenta morada y blanca: Estudio de propiedades térmicas, tecnológicas y morfológicas

UNIVERSIDAD NACIONAL DE COLOMBIA

José Trujillo-Ccanahuire[1], Elizabeth S. Ordoñez[2], Darlym Reategui[3] and Melchor Soria Iturri[1]*

ABSTRACT

Keywords:
Food industry
Gelatinization
Microstructure
Taro

The high demand for starch in the food industry drives the search for new alternative sources for extraction. In this regard, *Colocasia esculenta* (L.) Schott, an edible root, is a promising alternative source for starch extraction. This study focused on correlating the technological and thermal properties with the microstructure and size distribution of starch from white and purple varieties. Starch granules with high thermal stability (132-258.3 °C) and good digestibility based on granule size (0.79-4.05 μm) were obtained. It was demonstrated that larger starch granules exhibit higher water absorption capacity (WAC) (139±0.53%). Moreover, the increase in WAC results in a higher gelatinization temperature (76.1±0.3 °C), which is favorable as it allows the use of this starch in food processing at high temperatures.

RESUMEN

Palabras clave:
Industria de alimentos
Gelatinización
Microestructura
Taro

La alta demanda de almidón en la industria alimentaria provoca la búsqueda de nuevas fuentes alternativas para su extracción. En este sentido, *Colocasia esculenta* (L.) Schott es una raíz comestible que demuestra ser una buena fuente alternativa para la extracción de almidón. Este estudio se centró en relacionar las propiedades tecnológicas y térmicas con la microestructura y la distribución de tamaño del almidón de las variedades blanca y morada. Se obtuvieron gránulos de almidón con una alta estabilidad térmica (132-258,3 °C) y buena digestibilidad basada en el tamaño de los gránulos (0,79-4,05 μm). Se demostró que los gránulos de almidón más grandes originan mayor capacidad de absorción de agua (WAC) (139±0,53%), además el aumento de WAC genera una mayor temperatura de gelatinización (76,1±0,3 °C), este comportamiento es favorable, pues permite el uso de este almidón en el procesamiento de alimentos a altas temperaturas.

[1]Laboratorio Central de Investigación - Universidad Nacional Agraria de la Selva, Tingo María, Perú. jose.trujillo@unas.edu.pe ,
 soriamelchor127@gmail.com
[2]Departamento académico de Ciencia y Tecnología de Alimentos - Facultad de Ingeniería en Industrias Alimentarias, Universidad Nacional Agraria
 de la Selva, Tingo María, Perú. Elizabeth.ordonez@unas.edu.pe
[3]Biocentro - Universidad Nacional Agraria de la Selva, Tingo María, Perú. Darlym.reategui@unas.edu.pe
*Corresponding author

Global production of native starch is projected to reach 156.5 million tons by 2025, driven primarily by its extensive use in the food industry (Compart et al. 2023). However, traditional sources such as maize, potato, wheat, cassava, and sweet potato are being overexploited, highlighting the urgent need to investigate new botanical sources of starch (Singh et al. 2024). Research and characterization of novel or alternative starches could alleviate pressure on these limited sources.

Taro (*Colocasia esculenta* L.), a perennial herbaceous plant native to Asia and widespread in tropical and subtropical regions of the Americas has garnered increasing interest due to its technological and nutritional properties. Thriving in climates with annual precipitation between 1,800 and 2,500 mm and temperatures ranging from 12 to 35 °C, taro benefits from high solar luminosity (Nagar et al. 2021; Gupta et al. 2023). The edible corm of taro, which can be spherical, ellipsoidal, or conical in shape, typically contains 27% starch on a dry weight basis, with starch granules ranging from 1 to 6.5 µm (Legesse and Bekele 2021; Huang et al. 2024). Its high moisture and carbohydrate content promotes microbial activity, leading to post-harvest losses. Although research has been conducted on taro, most of it has focused on the characterization of fresh corms, with less attention given to the study of taro flour and starch (Boahemaa et al. 2024).

Starch, owing to its functional properties and diverse applications in the industry, stands out as the most commercially significant carbohydrate. These properties are closely linked to the composition, morphology, and molecular structure of amylose and amylopectin within starch granules, factors influenced by genetic, agronomic, and environmental conditions (Saraiva et al. 2020; Choque-Quispe et al. 2024). Technological properties assessed for starches in the food industry include gelatinization, solubility index, swelling capacity, water absorption capacity, syneresis/retrogradation, and emulsification capacity (Hui et al. 2024). Understanding these functional properties is critical for predicting starch behavior when incorporated into food products. Marboh and Mahanta (2021) highlighted the interrelationship between these technological properties. For instance, higher water absorption capacity correlates with reduced syneresis, thereby enhancing stability during the freezing and thawing

cycles of foods. Additionally, gelatinization alters the starch structure, leading to enhanced water separation in certain starches post-freezing and thawing (Moorthy et al. 2024). In Peru, particularly in the Huánuco region, the climatic conditions are favorable for the cultivation of taro, where both white and purple varieties are grown. However, the lack of scientific studies on the technological properties of taro has limited its economic exploitation. The aim was to study the morphology, color, techno-functional properties, and thermal behavior of starch extracted from taro (white and purple).

MATERIALS AND METHODS
This study was carried out in the Laboratorio Central de Investigación at the UNAS, located in the city of Tingo María, Rupa Rupa district, Leoncio Prado province, Huánuco region, Peru which is geographically located at 9°17'08'' south latitude and 75°59'52'' west longitude, at a height of 660 meters above sea level (masl), with a relative humidity of 80%, and an average annual temperature of 25 °C.

Raw material
Approximately 5 kg of fresh roots from the two taro varieties, white and purple, were collected from the CIPTALD (Figure 1); geographically situated at the coordinates: 9°51'' south longitude and 75°00'' longitude, in the Huánuco department (Peru). For the identification of the varieties, a cross-sectional cut was made in the roots to identify the color of the pulp, The purple variety was coded as **PTS**, and the white variety as **WTS**.

Starch extraction
The extraction was done according to the methodology of Naidoo et al. (2015). The roots were selected according to their variety and the first washing was done to eliminate impurities. Later the roots were peeled, and a second washing using distilled water was done, then the pulp was cut into 3 mm thick slices. These slices were dried at 50 °C for 8 h in an electric stove (MMM Group, EC 222 ECO, Germany), then the dry matter was ground and sifted (mesh=180 µm). Distilled water was added to the powder that was obtained at a proportion of 1:10 (powder mass: distilled water mass) at room temperature, and it was put in constant agitation for 6 h. Then it was left to sediment for 24 h, and later it was centrifuged at 14,000 g for 20
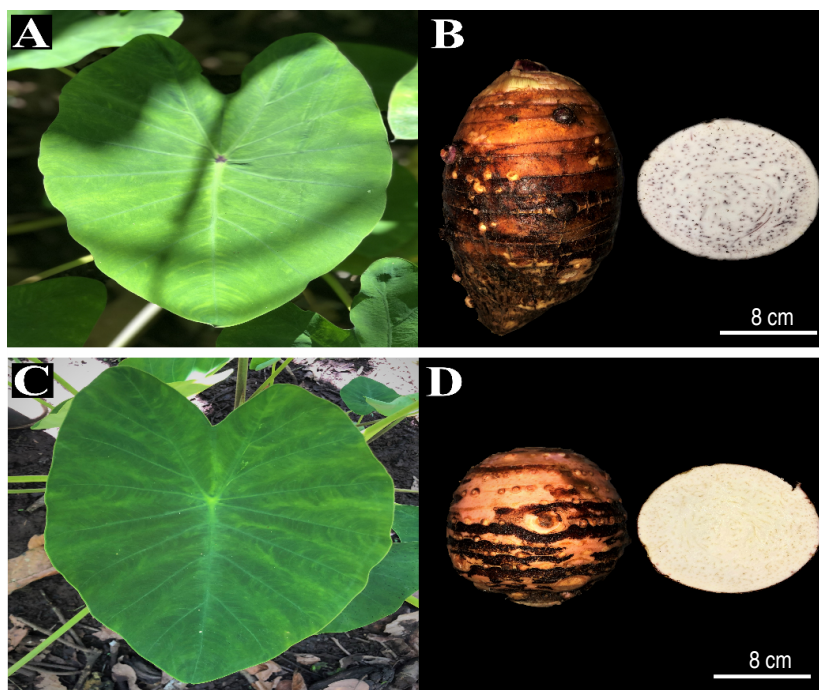
Figure 1. Plant and root. PTS (A, B) and WTS (C, D).

min (HETTICH, MIKRO 22 R, Germany). Finally, the solid fraction was dried at 50 °C for 24 h and the starch obtained was packaged in glass recipients with a screw-on top.

Analysis of the starch microstructure
The methodology described by Liu et al. (2018) was used, and the microstructures were observed using a scanning electron microscope (SEM) (Phenom-World B.V., Phenom ProX, Netherlands). The starches were fixed to the aluminum specimen holders with carbon tape, and they were covered with a gold film in a metallizer (Leica, EM ACE200, USA) for 5 min, with a 5 nm thickness. The micrographs were observed with increments from 4,000 and 4,500x, with an acceleration voltage of 15 kV while the images were obtained.

Chromaticity analysis
The color measurements were done using a colorimeter (Konica Minolta, Chroma meters CR-400, Japan); the basis for the measures was: luminosity (L*), red-green chroma (a*), and yellow-blue chroma (b*). The measurements were taken by placing the starches in a glass cell, focalizing the sources of the light, and covering the base of the glass cell with a white plaque.

The whiteness index (WI) was determined using Equation 1, reported by Guo et al. (2019).

$$WI = 100 - \sqrt{(100 - L^*)^2 + (a^*)^2 + (b^*)^2} \qquad (1)$$

Analysis of the starch technological properties
Water absorption capacity (WAC)
The method proposed by Ashri et al. (2014) was utilized. For this, a suspension of starch with distilled water was prepared in a proportion of 1:15 (starch mass: water volume); it was agitated for 1 h and was centrifuged at 1,006 g for 15 min to eliminate the supernatant. The mass of the wet starch was recorded, and the WAC was expressed as a percentage using Equation 2.

$$WAC(\%) = \frac{\text{wet starch mass (g)}}{\text{dry starch mass (g)}} \times 100 \qquad (2)$$

Solubility in cold water (S)
This was estimated according to the method recommended by Zhu et al. (2017a). To do this, the starch was dispersed in water at a concentration of 1% (w/w) and it was agitated at 100 rpm for 30 min at 25 °C, utilizing a magnetic agitator (Ultra-Turrax, IKA®, USA);

Rev. Fac. Nac. Agron. Medellín 77(3): 10887-10897. 2024

10889

later the mix was centrifuged at 1,372 g for 10 min. The supernatant was poured onto a plaque and was dried at 105 °C for 4 h; finally, the dissolved solids were weighed, and the solubility was expressed as a percentage, according to Equation 3:

$$S(\%) = \frac{\text{dry supernatant mass (g)}}{\text{dispersed starch mass (g)}} \times 100 \qquad (3)$$

Stability during freezing-thawing (Si)
The methodology described by Salgado-Ordosgoitia et al. (2018) was utilized. For this, a starch suspension was prepared at 5% (w/v); this was heated at 95 °C for 30 min in a water bath with constant agitation (MEMMERT, WNB 22, Germany). The gel obtained was cooled at 26±2 °C, from which, 2 g was placed in centrifuge tubes and was stored at 4 °C for 24 h. Later, they were frozen (LG, GR-5392QLC, South Korea) at -20 °C for 48 h. The thawing was done at 25 °C for 3 h and the samples were centrifuged at 2,360 g for 15 min. Finally, the separated water was weighed and the percentage of syneresis was calculated using Equation 4:

$$Si(\%) = \frac{\text{mass of the separated liquid water(g)}}{\text{mass of the starch from the gel (g)}} \qquad (4)$$

Analysis of the starch thermal behavior
Thermal stability (TG/DTG)
For the thermogravimetric analysis, a calorimeter was used (SETARAM, Labsys EVO robot option, USA), following the methodology described by Londoño-Restrepo et al. (2014). For this, 5 mg of starch was weighed in an aluminum crucible and the samples were heated from 25 to 550 °C; the best heating velocity was 10 °C min^{-1} with a nitrogen flow of 50 mL min^{-1}. The mass loss was processed using Calisto software incorporated into the equipment. The maximum temperature for each thermal event was calculated on the DTG curve.

Analysis of gelatinization by DSC
The method proposed by Iturri et al. (2021) was used. For this, 10 mg of starch was weighed in an aluminum crucible, and to create the suspension, distilled water was added at a 1:3 ratio (starch mass: distilled water mass). The crucible was sealed and stored between 25 and 27 °C for 1 h. The calorimeter (SETARAM, Labsys EVO robot option, USA) was calibrated with indium (99.99%

purity, fusion temperature of 126.63 °C). The heating was programmed from 25 to 110 °C; the best heating velocity was 5 °C min^{-1} in an inert environment with a nitrogen flow of 30 mL min^{-1}. The gelatinization temperatures (onset, To; peak, Tp; and conclusion, Tc) and gelatinization enthalpy (ΔH) were calculated with the Calisto SETARAM software.

Statistical Analysis
All analyses were performed in triplicate and the values are reported as mean ± standard deviation. The t-student statistical analysis with paired variables proposed by Flores-Ruiz et al. (2017) was utilized to evaluate if a statistically significant difference existed between the two **taro varieties** concerning the size, WAC, S, Si, WI, and thermal behavior of the starch granules. The statistical test was performed using the Statistical software version 13 (StatSoftInc, Tulsa, OK, USA.) with 95% confidence.

RESULTS AND DISCUSSION
Morphological characterization and size distribution
The starches from both varieties of taro proved to be similar morphologically, presenting characteristics of irregular polyhedral granules with central cavities (Figure 2 and Table 1); this same morphology was also reported by Andrade et al. (2017) and Martins et al. (2020) in *C. esculenta* starch granules. Nonetheless, this morphological similarity is not common among the starch sources, for example, Zhu (2016) found differences in the morphology of starches due to the genetic variations between *Alocasia macrorrhiza, Amorphophallus campanulatus, Cyrtosperma merkusii,* and *Xanthosoma sagittifolium.*

The granules of PTS and WTS had similar size ranges in the inferior as well as superior limits; moreover, there was no proven significant statistical difference between them for the average arithmetic size (Table 1), nor did they prove to have the same size distribution (Figures 2C and 2D). For granules of PTS, a large percentage was in the size intervals of 1.13–1.47 µm (22.1%) and 1.81–2.14 µm (20.7%), while for granules of WTS, the greatest percentage was found in the size intervals of 1.21–1.57 µm (20.7%), 1.57–1.93 µm (23.6%) and 1.93–2.29 µm (18.6%). The difference in the size distribution between the PTS and WTS also was evidenced by the values difference of the diameter representative of the sample (D$_{[3,2]}$). The interval for the diameters of the starch granules (Table 1) was within the range reported by Zhu et

Table 1. Morphologic characterization, size, chromaticity, technological and thermal properties of taro starch.

Morphology and Size	PTS*	WTS*
Form	Polyhedric with cavities and roundedness	Polyhedric with cavities and fissures
Size range (µm)	0.79-3.84	0.85-4.05
Average (µm)	1.97 ± 0.66^a	1.90 ± 0.63^a
$D_{[3,2]}$ (µm)	2.41	2.31
Chromaticity		
L^*	99.72 ± 0.13^a	96.43 ± 0.08^b
a^*	-0.59 ± 0.01^b	0.29 ± 0.02^a
b^*	8.87 ± 0.04^a	8.92 ± 0.05^a
WI	91.10 ± 0.04^a	90.39 ± 0.06^b
Technological properties		
WAC (%)	127.8 ± 1.61^b	1.39 ± 0.53^a
S (%)	1.33 ± 0.21^b	3.20 ± 0.12^a
Si (%)	6.92 ± 1.22^a	6.24 ± 1.13^a
Thermogravimetry	$\Delta T; (\% \ m \ m^{-1})$	$\Delta T; (\% \ m \ m^{-1})$
Δm_1 (stage 1)	30-139 °C; (7.9%)	30.3-132.8 °C; (7.1%)
Stability (stage 2)	139-258.3 °C; (0.0%)	132.8-229.6 °C; (0.0%)
Δm_2 (stage 3)	258.3-360.1 °C; (54.8%)	229.6-380.0 °C; (64.4%)
Δm_3 (stage 4)	362.4-554.3 °C; (10.0%)	381.7-554.1 °C; (7.4%)
Gelatinization (DSC)		
T_o (°C)	74.9 ± 0.4^b	76.1 ± 0.3^a
T_p (°C)	78.6 ± 0.2^b	81.5 ± 0.5^a
T_c (°C)	83.2 ± 0.3^b	88.0 ± 0.7^a
ΔH (J g^{-1})	2.7 ± 0.0^b	3.1 ± 0.1^a

Values in the same row with different super indices have statistically significant differences according to the t-student test ($P<0.05$). PTS*: Purple taro starch, WTS*: White taro starch. $D_{[3,2]}$: Sauter diameter; WI: Whiteness Index; WAC: Water retention capacity; S: Solubility; Si: Syneresis; ΔT: Thermal decomposition temperature range; % m m^{-1}: Percentage mass loss.

al. (2017b) (0.39–5.02 µm) in starch granules in three *C. esculenta* varieties originating from the Jiangsu province of China; in that study, the difference in granule sizes was also subjected to the *C. esculenta* varieties, as reported by Zhu (2016). According to Aboubakar et al. (2008), the size of starch granules that are highly digestible for kids and the elderly is between $3 \le d \le 20$ µm, which indicates that PTS and WTS are highly metabolized.

The size distribution of the starch granules had an important effect on the WAC since large granules have greater swelling causing greater water absorption, this can be visualized in Figure 2D, where the granules of WTS had a high percentage of larger granules and generated an elevated WAC (Table 1).

The increase in the WAC influenced the delay of the gelatinization process, increasing the typical temperatures for the process; for example, for the granules of WTS, the WAC was 139% with To, Tp, and Tc greater than for the granules of WTS which had a WAC of 127.8%. Also, the gelatinization enthalpy (Table 1) was affected by the increase in the WAC; this behavior was also reported by Calle et al. (2021) in starch of *Xanthosoma sagittifolium*.

Whiteness index
This parameter is related to starch purity; the chromaticity values are in Table 1. According to Sit et al. (2014), a value superior to 90.0 for this index reflects a high purity for the extracted starch. Consequently, the starches from the two varieties of this study (PTS and WTS) had
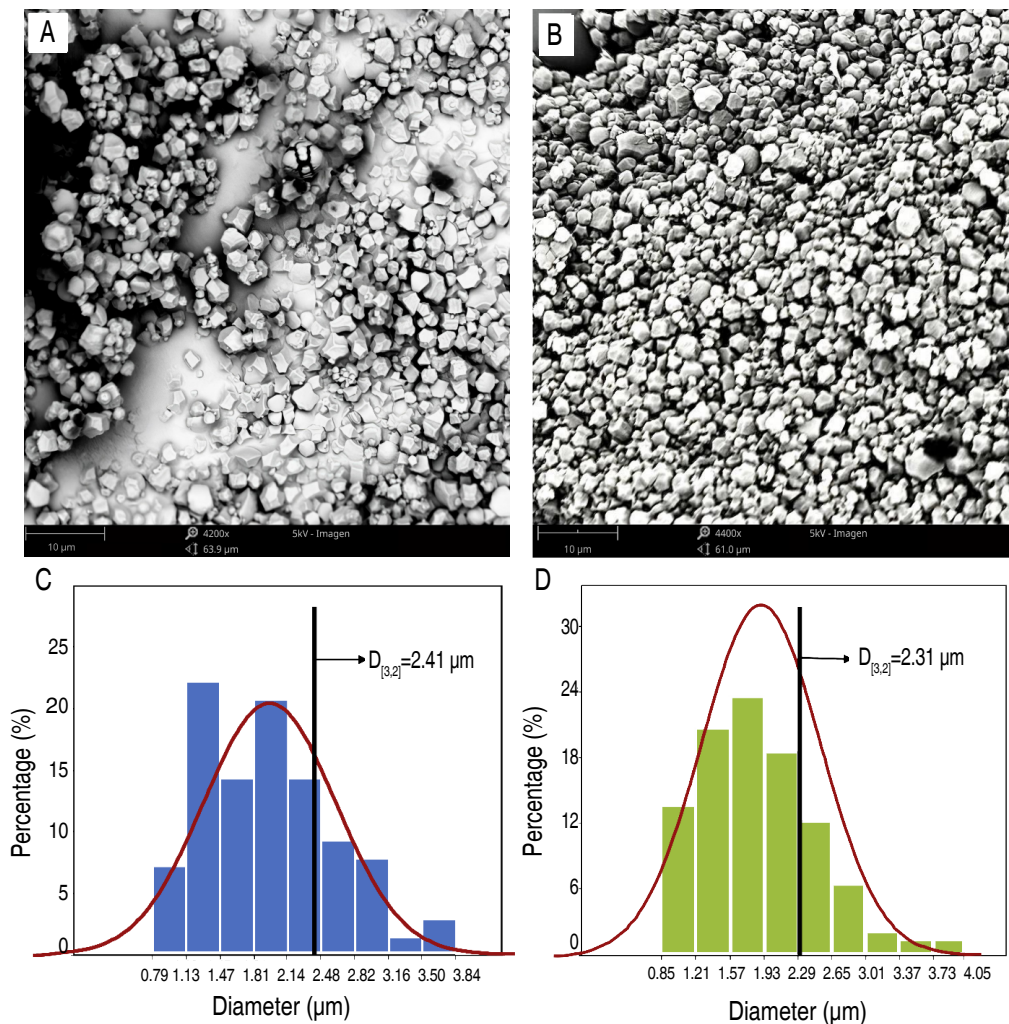
Rev. Fac. Nac. Agron. Medellín 77(3): 10887-10897. 2024

10891

Figure 2. Morphology and size distribution of the starch granules. PTS (A, C) and WTS (B, D).

acceptable purities for their use in the food industry, as mentioned by Guo et al. (2019), given that they are framed within the acceptable range (PTS: WI=91.10±0.04 and WTS: WI=90.39±0.06). The differences in the a^* chroma between the varieties were due to the intensity of the non-enzymatic browning (Maillard reaction), which is related to the humidity content of the starch (Kim et al. 2013; Deka and Sit 2016). For example, the TG analysis for the PTS revealed a higher humidity, of 7.9%, with $a^*=-0.59$, and in the WTS it was 7.1% with $a^*=0.29$. Greater humidity content generates a greater WI due to the water reflection effect; this was corroborated by the data (PTS: 7.9% with WI=91.10 and WTS: 7.1% with WI=90.39).

On the other hand, a greater amylopectin content generates a greater opacity (less luminosity) in the starch, as was mentioned by Bultosa and Taylor (2003); this was corroborated by the DTG analysis (Figure 3), where the PTS presented a more acute area under the degradation curve and it had a greater luminosity, which is characteristic of the lower amylopectin content.

Technological properties
Water absorption capacity
To establish the starch functionality when submitted to the thermal process it is necessary to quantify the WAC, which allows for the prediction of the capacity to be used as an emulsifier and in the formation of gels. According
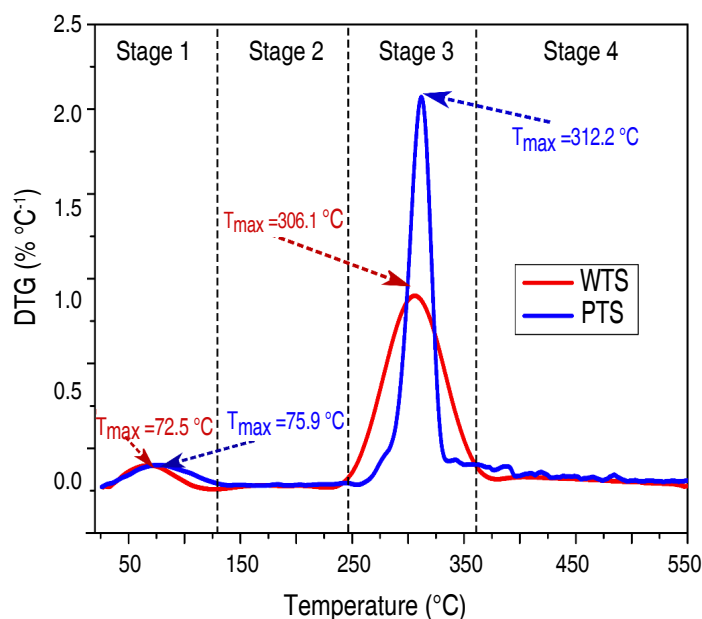
Figure 3. DTG of the starch from purple (PTS) and white taro (WTS).

to the results of the WAC, a statistical difference existed ($P<0.05$) between the PTS with 1.28 g g^{-1} (127.8%) and the WTS with 1.39 g g^{-1} (139.0%). These values were inferior to those reported by Calle et al. (2021) for *Colocasia* spp. Flour (1.75±0.15 g g^{-1}); this difference is related to the larger average size of the granules reported by these authors (117.24±8.62 µm), which influences the greater WAC. The differences in the WAC between the PTS and WTS can also be explained because of the white variety's high percentage of larger-sized granules (Figure 2). On the other hand, the relationship proposed by Amon et al. (2014), as it presented a greater WAC, it is possible to consider that the WTS presents a greater quantity of hydrophilic constituents on the external surface of the granule (polysaccharides).

Solubility in cold water
Solubility is the capacity that the starch has to bond with the water, indicating the degree of association between amylose-amylopectin, crystallinity, and granule size (Rafiq et al. 2015; Wang et al. 2018). The greatest percentage of solubility was for the WTS, in comparison to the PTS; this is explained due to the greater amylopectin content (branched chain, more hydrogen bonds) (Figure 3) and

the smaller granule size of the starch ($D_{[3,2]}$=2.31 µm), making that the water gets in the starch granules. Studies done for other starch sources reported similar values for solubility, such as 2.67–3.86% for three varieties of *C. esculenta* (Falade and Okafor 2013), 1.25% for *Dioscorea alata* L., 3.70% for *Manihot sculenta*, and 2.97% for *Solanum tuberosum* (Alvis et al. 2008).

Stability during freezing-thawing
This parameter is important because it predicts a possible microbiological degradation (increase in water activity) and decreases in the sensory quality of the frozen foods after thawing due to the thermal variations, and the water changes phase, provoking the liberation of liquid water during storage (Gupta et al. 2021).

During the freezing and thawing process of the starches, the phenomenon evidenced is "syneresis," which is related to the loss of water due to exudation. The syneresis values did not reveal a statistical difference (Table 1); this can be attributed to the fact that during the freezing-thawing process, both samples had the same size of ice crystals, analogous to the average granule sizes of the starch (Table 1), and the same amylose-amylopectin crystalline structure as also reported by Liu et al. (2019).

Rev. Fac. Nac. Agron. Medellín 77(3): 10887-10897. 2024

10893

Thermogravimetry (TG/DTG)

Table 1 shows the percentages of mass loss and the degradation temperature intervals, and in Figure 4 the TG and DTG are recorded with the stages of thermal degradation. The principal event of the first stage was water loss and volatile compounds; likewise, according to Liu et al. (2010), during this stage, there is rapid dehydration and decomposition of glucose hydroxyl groups which form water molecules, which are evaporated in this same stage of decomposition. The PTS presented a greater percentage of mass loss in comparison to the WTS, and the maximum decomposition temperatures were 75.9 and 72.5 °C, respectively (Figure 3). Andrade et al. (2017) and Elmi Sharlina et al. (2017), found similar weight loss percentages in the starch associated with the first stage.

In the second stage, the starch granules showed thermal stability, with no mass loss occurring (Table 1 and Figure 4). The PTS presented greater thermal stability in this stage, reaching a ∆T range of 119.3 °C; while for the WTS, the ∆T range was 96.8 °C. This behavior is explained by the greater amylose content present in the PTS (Figure 3); curve with a slim base and greater height in stage 3, which generated a higher internal energy demand during the thermal destructuring in this stage. Moreover, the amylose-amylopectin proportion is 20/80, as reported by Singla et al. (2020), and the amylose has a linear chemical structure that generates greater resistance to thermal degradation. According to Martins et al. (2020), the differences in the temperature range during this stage are related to the crystallinity of the starch as a function of the disposition of amylose and amylopectin; these authors reported that the average typical temperature at the end of this stage is 251.9 °C; in this study, similar temperatures were found.

Londoño-Restrepo et al. (2014) indicated that the widening of the peak with a lower height in the third stage of thermal decomposition corresponds to a greater amylopectin content in the starch (Figure 3). In the third stage, a greater decomposition occurred, related to the loss of mass for the majority compound (amylose for the PTS and amylopectin for WTS); there was also a difference in the
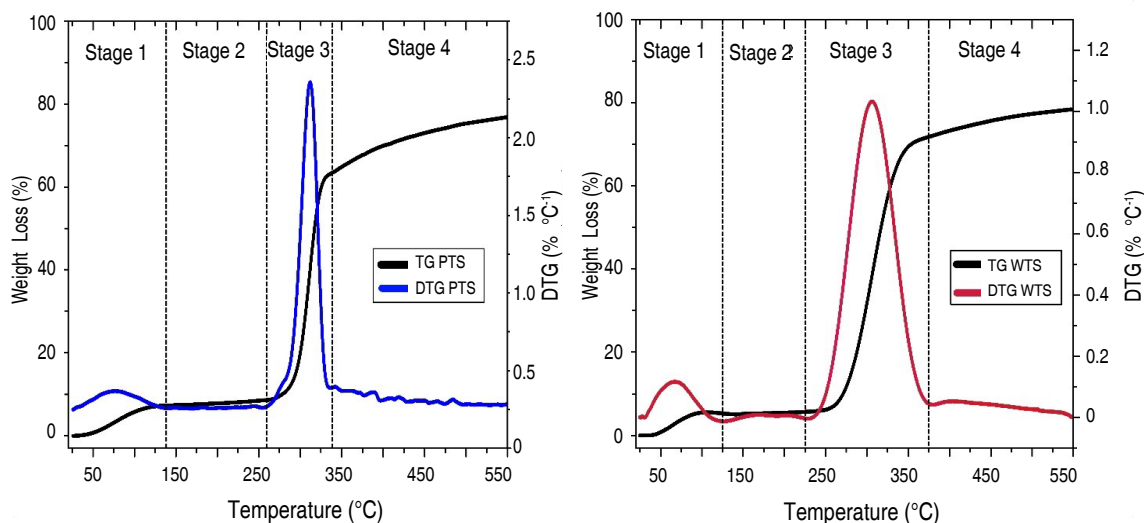

Figure 4. TG/DTG thermogram of starch from purple (PTS) and white (WTS) Taro.

degradation temperature range of the starches (Figure 4 and Table 1). Studies related to the thermal behavior of the *C. esculenta* starch revealed similar values in the loss of mass and temperature range for this stage; the same which are associated in this stage with the degradation of amylose and the breaking of the amylopectin chain (Liu et al. 2010; Andrade et al. 2017; Martins et al. 2020).

The fourth stage corresponded to the formation of inert carbonaceous waste and a slow decomposition

existed due to the formation of CO_2 originating from the separation of oxygen from the amylose-amylopectin complex; the final waste from the pyrolysis process, with an absence of external oxygen flow, reached 27.3% for the PTS and 21.1% for WTS; according to Mukurumbira et al. (2017) and Xu et al. (2014), this difference can be attributed to the crystalline structure and the increase of the intermolecular interactions during the thermal decomposition of the starch's polymeric structure.

Analysis of the gelatinization by DSC
The PTS and WTS presented a zone for endothermal energy exchange, corresponding to the gelatinization process (Figure 5). The typical temperatures for the endothermal peak, To, Tp (peak temperature), and Tc revealed significant statistical differences between the samples (Table 1). On top of presenting the greater amylose content, the WTS also had a greater Tp; which generated a greater energy demand (3.1 J g^{-1}), given that the amylose acts as a dilutant (greater absorption of water molecules in the starch granules during the gelatinization). Coronell-Tovar et al. (2019) and Elmi Sharlina et al. (2017), also indicated that the different typical temperatures and the enthalpy during the gelatinization were associated with the amylose and amylopectin content, crystallinity degree, morphology, size distribution, and the water absorption capacity of the starch granules. The gelatinization enthalpy presented statistical differences between the PTS and the WTS (Table 1); these values for the enthalpy were similar to those reported by Jiang et al. (2012) in starch granules of *C. esculenta* and *D. bulbifera*, respectively.
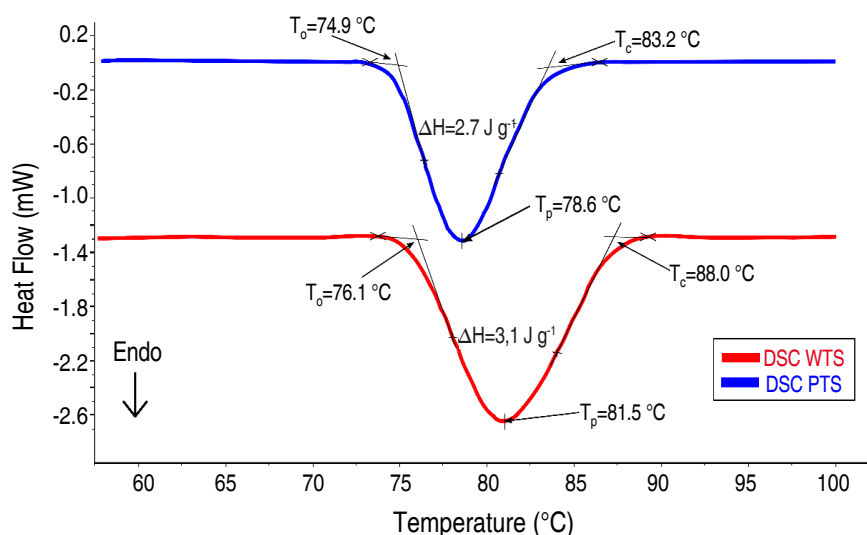

Figure 5. Endothermic peak during gelatinization of purple (PTS) and white (WTS) taro starches.

CONCLUSION
The comparative study of purple (PTS) and white (WTS) sweet potato starches revealed significant similarities and differences in their morphological, technological, and thermal properties. Both varieties exhibited similar morphology, with polyhedral granules and cavities; however, WTS stood out for having larger granules, resulting in higher water-holding capacity (WHC) and opacity. Thermogravimetry showed higher thermal stability for PTS, whereas WTS differential scanning calorimetry exhibited a higher peak temperature (Tp) and greater gelatinization enthalpy, suggesting higher energy requirements. These findings underscore the importance of considering the specific characteristics of each starch variety for effective application in the food industry and other technological areas.

ACKNOWLEDGMENTS

REFERENCES

Aboubakar, Njintang YN, Scher J and Mbofung CMF (2008) Physicochemical, thermal properties and microstructure of six varieties of taro (*Colocasia esculenta* L. Schott) flours and starches. Journal of Food Engineering 86: 294–305. https://doi.org/10.1016/j.jfoodeng.2007.10.006

Alvis A, Vélez CA, Villada HS and Rada-Mendoza M (2008) Análisis físico-químico y morfológico de almidones de ñame, yuca y papa y determinación de la viscosidad de las pastas. Información Tecnológica 19: 19–28. https://doi.org/10.4067/s0718-07642008000100004

Amon AS, Soro RY, Assemand EF et al (2014) Effect of boiling time on chemical composition and physico-functional properties of flours from taro (*Colocasia esculenta* cv fouê) corm grown in Côte d'Ivoire. Journal of Food Science and Technology 51: 855–864. https://doi.org/10.1007/s13197-011-0578-7

Andrade LA, Barbosa NA and Pereira J (2017) Extraction and properties of starches from the non-traditional vegetables Yam and Taro. Polimeros 27: 151–157. https://doi.org/10.1590/0104-1428.04216

Ashri A, Yusof MSM, Jamil MS et al (2014) Physicochemical characterization of starch extracted from Malaysian wild yam (*Dioscorea hispida* Dennst.). Emirates Journal of Food and Agriculture 26: 652–658. https://api.semanticscholar.org/CorpusID:12901363

Boahemaa LV, Dzandu B, Amissah JGN et al (2024) Physico-chemical and functional characterization of flour and starch of taro (*Colocasia esculenta*) for food applications. Food Humanity 2: 100245. https://doi.org/10.1016/j.foohum.2024.100245

Bultosa G and Taylor JRN (2003) Chemical and physical characterisation of grain tef [*Eragrostis tef* (Zucc.) Trotter] starch granule composition. Research Paper. Starch 55: 304–312. https://doi.org/10.1002/star.200390065

Calle J, Benavent-Gil Y and Rosell CM (2021) Use of flour from cormels of *Xanthosoma sagittifolium* (L.) Schott and *Colocasia esculenta* (L.) Schott to develop pastes foods: Physico-chemical, functional and nutritional characterization. Food Chemistry 344: 128666. https://doi.org/10.1016/j.foodchem.2020.128666

Choque-Quispe D, Obregón Gonzales FH, Carranza-Oropeza MV et al (2024) Physicochemical and technofunctional properties of high Andean native potato starch. Journal of Agriculture and Food Research 15: 100955. https://doi.org/10.1016/j.jafr.2023.100955

Compart J, Singh A, Fettke J and Apriyanto A (2023) Customizing starch properties: A review of starch modifications and their applications. Polymers (Basel) 15: 3491. https://doi.org/10.3390/polym15163491

Coronell-Tovar DC, Chávez-Jáuregui RN, Bosques-Vega Á and López-Moreno ML (2019) Characterization of cocoyam (*Xanthosoma* spp.) corm flour from the nazareno cultivar. Food Science and Technology 39: 349–357. https://doi.org/10.1590/fst.30017

Deka D and Sit N (2016) Dual modification of taro starch by microwave and other heat moisture treatments. International Journal of Biological Macromolecules 92: 416–422. https://doi.org/10.1016/j.ijbiomac.2016.07.040

Elmi Sharlina MS, Yaacob WA, Lazim AM et al (2017) Physicochemical Properties of Starch from *Dioscorea pyrifolia* tubers. Food Chemistry 220: 225–232. https://doi.org/10.1016/j.foodchem.2016.09.196

Falade KO and Okafor CA (2013) Physicochemical properties of five cocoyam (*Colocasia esculenta* and *Xanthosoma sagittifolium*) starches. Food Hydrocolloids 30: 173–181. https://doi.org/10.1016/j.foodhyd.2012.05.006

Flores-Ruiz E, Miranda-Novales M and Villasís-Keever M (2017) El protocolo de investigación VI: cómo elegir la prueba estadística adecuada. Estadística inferencial. Revista Alergia México 64: 364–370. https://doi.org/10.29262/ram.v64i3.304

Guo J, Kong L, Du B and Xu B (2019) Morphological and physicochemical characterization of starches isolated from chestnuts cultivated in different regions of China. International Journal of Biological Macromolecules 130: 357–368. https://doi.org/10.1016/j.ijbiomac.2019.02.126

Gupta RK, Guha P and Srivastav PP (2023) Effect of high voltage dielectric barrier discharge (DBD) atmospheric cold plasma treatment on physicochemical and functional properties of taro (*Colocasia esculenta*) starch. International Journal of Biological Macromolecules 253: 126772. https://doi.org/10.1016/j.ijbiomac.2023.126772

Gupta V, Thakur R and Das AB (2021) Effect of natural deep eutectic solvents on thermal stability, syneresis, and viscoelastic properties of high amylose starch. International Journal of Biological Macromolecules 187: 575–583. https://doi.org/10.1016/j.ijbiomac.2021.07.099

Huang G, Wang F, Yang R, Wang ZC, Fang Z et al (2024) Characterization of the physicochemical properties of Lipu *Colocasia esculenta* (L.) Schott starch: A potential new food ingredient. International Journal of Biological Macromolecules 254: 127803. https://doi.org/10.1016/j.ijbiomac.2023.127803

Hui G, Zhu P and Wang M (2024) Structure and functional properties of taro starch modified by dry heat treatment. International Journal of Biological Macromolecules 261:129702. https://doi.org/10.1016/j.ijbiomac.2024.129702

Iturri MS, Calado CMB and Prentice C (2021) Microparticles of Eugenia stipitata pulp obtained by spray-drying guided by DSC: An analysis of bioactivity and *in vitro* gastrointestinal digestion. Food Chemistry 334: 127557.https://doi.org/10.1016/j.foodchem.2020.127557

Jiang Q, Gao W, Li X et al (2012) Characterizations of starches isolated from five different Dioscorea L. species. Food Hydrocolloids 29: 35–41. https://doi.org/10.1016/j.foodhyd.2012.01.011

Kim J, Ren C and Shin M (2013) Physicochemical properties of starch isolated from eight different varieties of Korean sweet potatoes. Starch 65: 923–930. https://doi.org/10.1002/star.201200217

Legesse T and Bekele T (2021) Evaluation of improved taro (*Colocasia esculenta* (L.) Schott) genotypes on growth and yield performance in North-Bench woreda of Bench-Sheko zone, South-Western Ethiopia. Heliyon 7: e08630. https://doi.org/10.1016/j.heliyon.2021.e08630

Liu C, An F, He H et al (2018) Pickering emulsions stabilized by compound modified areca taro (*Colocasia esculenta* (L.) Schott) starch with ball-milling and OSA. Colloids Surfaces A: Physicochemical Engineering Aspects 556: 185–194. https://doi.org/10.1016/j.colsurfa.2018.08.032

Liu X, Yu L, Xie F et al (2010) Kinetics and mechanism of thermal decomposition of cornstarches with different amylose/amylopectin ratios. Starch 62: 139–146. https://doi.org/10.1002/star.200900202

Liu Y, Yang L, Ma C and Zhang Y (2019) Thermal behavior of sweet potato starch by non-isothermal thermogravimetric analysis. Materials (Basel) 12: 699. https://doi.org/10.3390/ma12050699

Londoño-Restrepo SM, Rincón-Londoño N, Contreras-Padilla M et al (2014) Physicochemical, morphological, and rheological characterization of *Xanthosoma robustum* Lego-like starch. International Journal of Biological Macromolecules 65: 222–228. https://doi.

org/10.1016/j.ijbiomac.2014.01.035

Marboh V and Mahanta CL (2021) Physicochemical and rheological properties and in vitro digestibility of heat moisture treated and annealed starch of sohphlang (*Flemingia vestita*) tuber. International Journal of Biological Macromolecules 168: 486–495. https://doi.org/10.1016/j.ijbiomac.2020.12.065

Martins A, Beninca C, Bet CD et al (2020) Ultrasonic modification of purple taro starch (*Colocasia esculenta* B. Tini): structural, psychochemical and thermal properties. Journal of Thermal Analysis and Calorimetry 142: 819–828. https://doi.org/10.1007/s10973-020-09298-3

Moorthy SN, Sajeev MS and Anish RJ (2024) Chapter 14 - Functionality of tuber starches. Starch in Food 14: 327–375. https://doi.org/10.1016/b978-0-323-96102-8.00022-x

Mukurumbira A, Mariano M, Dufresne A et al (2017) Microstructure, thermal properties and crystallinity of amadumbe starch nanocrystals. International Journal of Biological Macromolecules 102: 241–247. https://doi.org/10.1016/j.ijbiomac.2017.04.030

Nagar CK, Dash SK, Rayaguru K et al (2021) Isolation, characterization, modification and uses of taro starch: A review. International Journal of Biological Macromolecules 192: 574–589. https://doi.org/10.1016/j.ijbiomac.2021.10.041

Naidoo K, Amonsou EO and Oyeyinka SA (2015) *In vitro* digestibility and some physicochemical properties of starch from wild and cultivated amadumbe corms. Carbohydrate Polymers 125: 9–15. https://doi.org/10.1016/j.carbpol.2015.02.066

Rafiq SI, Jan K, Singh S and Saxena DC (2015) Physicochemical, pasting, rheological, thermal and morphological properties of horse chestnut starch. Journal of Food Science and Technology 52: 5651–5660. https://doi.org/10.1007/s13197-014-1692-0

Salgado-Ordosgoitia RD, Rodríguez-Manrique JA, Cohen-Manrique CS and Mendoza-Ortega GP (2018) Characterization of the techno-functional properties of starch from purple yam (*Dioscorea alata*), Hawthorn yam (*Dioscorea rotundata*) and Diamante 22-type yam. DYNA 85: 143–152. https://doi.org/10.15446/dyna.v85n207.72869

Saraiva SC, da Silva AS, de Carvalho LH et al (2020) Morphological, structural, thermal properties of a native starch obtained from babassu mesocarp for food packaging application. Journal of Materials Research and Technology 9: 15670–15678. https://doi.org/10.1016/j.jmrt.2020.11.030

Singh AK, Lee M, Jang D and Lee YS (2024) Non-conventional starch nanoparticles: Novel avenues towards improving sustainability of the food packaging sector. Trends in Food Science & Technology 143: 104273. https://doi.org/10.1016/j.tifs.2023.104273

Singla D, Singh A, Dhull SB et al (2020) Taro starch: Isolation, morphology, modification and novel applications concern - A review. International Journal of Biological Macromolecules 163: 1283–1290. https://doi.org/10.1016/j.ijbiomac.2020.07.093

Sit N, Deka SC and Misra S (2014) Combined effect of ultrasound and enzymatic pretreatment on yield and functional properties of taro (*Colocasia esculenta*) starch. Starch 66: 959–967. https://doi.org/10.1002/star.201400085

Wang X, Reddy CK and Xu B (2018) A systematic comparative study on morphological, crystallinity, pasting, thermal and functional characteristics of starches resources utilized in China. Food Chemistry 259: 81–88. https://doi.org/10.1016/j.foodchem.2018.03.121

Xu Y, Sismour EN, Grizzard C et al (2014) Morphological, structural, and thermal properties of starch nanocrystals affected by different botanic origins. Cereal Chemistry 91: 383–388. https://doi.org/10.1094/CCHEM-10-13-0222-R

Zhu B, Liu J and Gao W (2017a) Process optimization of ultrasound-assisted alcoholic-alkaline treatment for granular cold water swelling starches. Ultrasonics Sonochemistry 38: 579–584. https://doi.org/10.1016/j.ultsonch.2016.08.025

Zhu F (2016) Structure, properties, and applications of aroid starch. Food Hydrocolloids 52: 378–392. https://doi.org/10.1016/j.foodhyd.2015.06.023

Zhu J, Zhang S, Zhang B et al (2017b) Structural features and thermal property of propionylated starches with different amylose/amylopectin ratio. International Journal of Biological Macromolecules 97: 123–130. https://doi.org/10.1016/j.ijbiomac.2017.01.033

Rev. Fac. Nac. Agron. Medellín 77(3): 10887-10897. 2024

10897